



**Michigan
Technological
University**

Michigan Technological University
Digital Commons @ Michigan Tech

Dissertations, Master's Theses and Master's Reports

2017

AIR INJECTION AS A SCOUR COUNTERMEASURE AT BRIDGE PIERS

Ravi Teja Reddy Tippireddy
Michigan Technological University, rtippire@mtu.edu

Copyright 2017 Ravi Teja Reddy Tippireddy

Recommended Citation

Tippireddy, Ravi Teja Reddy, "AIR INJECTION AS A SCOUR COUNTERMEASURE AT BRIDGE PIERS", Open Access Master's Thesis, Michigan Technological University, 2017.
<https://doi.org/10.37099/mtu.dc.etr/469>

Follow this and additional works at: <https://digitalcommons.mtu.edu/etr>



Part of the [Civil Engineering Commons](#), [Environmental Engineering Commons](#), [Geotechnical Engineering Commons](#), [Hydraulic Engineering Commons](#), [Other Civil and Environmental Engineering Commons](#), [Structural Engineering Commons](#), and the [Transportation Engineering Commons](#)

AIR INJECTION AS A SCOUR COUNTERMEASURE AT BRIDGE PIERS

By

Ravi Teja Reddy Tippireddy

A THESIS

Submitted in partial fulfillment of the requirements for the degree of

MASTER OF SCIENCE

In Civil Engineering

MICHIGAN TECHNOLOGICAL UNIVERSITY

2017

© 2017 Ravi Teja Reddy Tippireddy

This thesis has been approved in partial fulfillment of the requirements for the Degree of
MASTER OF SCIENCE in Civil Engineering.

Department of Civil and Environmental Engineering

Thesis Advisor: *Dr. Brian D. Barkdoll*

Committee Member: *Dr. Zhen Liu*

Committee Member: *Dr. Casey J. Huckins*

Department Chair: *Dr. Audra Morse*

Table of Contents

List of Figures	vii
List of Tables	ix
Acknowledgements	x
Abstract	xi
Chapter 1: Introduction	1
1.1. Introduction	1
1.1.1. Existing Countermeasures	2
1.1.2. Bubble Screen	6
1.2. Objective	8
Chapter 2: Procedure	9
2.1. Experimental Set up	9
2.1.1. Laboratory	9
2.1.2. Flume Setup	9
2.2. Experimental Procedure	16
2.3. Data Collection	16
2.4. Experiments	17
2.4.1. Scour Experiments	17
2.4.2. Dye Test	21
Chapter 3: Results	22
3.1. Rate of Scour:	22
3.2. Equilibrium Scour Depth	23
3.3. Centerline Scour Depth	24
3.4. Time to Equilibrium	26
3.5. Water Surface Profile	26

3.6. Bed Profile.....	28
3.7. Dye Test.....	36
Chapter 4: Conclusions.....	40
Chapter 5: Future Work.....	41
References.....	42

List of Figures

Figure 1. View of flume looking upstream. Features are described in the numbered list below	10
Figure 2. Schema of flume with sections	11
Figure 3. Steel diffuser pipe around the upstream half of the pier (looking downstream)	14
Figure 4. Rate of scour with varied air flow rate	23
Figure 5. Scour depth variation with change in air flow rate	24
Figure 6. Centerline bed elevation with varied air flow rate	25
Figure 7. Time to equilibrium with varied air flow rate	26
Figure 8. Water surface elevation with varied air flow rate	27
Figure 9. Bed Profile for the base case of $V_a/V_w = 0$. (Flow was from left to right. Contour interval was 1 cm)	28
Figure 10. Bed profile for $V_a/V_w = 7.14$. (Flow was from left to right. Contour interval was 1 cm)	29
Figure 11. Bed profile for $V_a/V_w = 21.41$. (Flow was from left to right. Contour interval was 1 cm)	29
Figure 12. Bed profile for $V_a/V_w = 35.69$. (Flow was from left to right. Contour interval was 1 cm)	30
Figure 13. Bed profile for $V_a/V_w = 49.96$. (Flow was from left to right. Contour interval was 1 cm)	30
Figure 14. Bed profile for $V_a/V_w = 57.10$. (Flow was from left to right. Contour interval was 1 cm)	31
Figure 15. Bed profile for $V_a/V_w = 64.24$. (Flow was from left to right. Contour interval was 1 cm)	31
Figure 16. Bed profile for $V_a/V_w = 71.37$. (Flow was from left to right. Contour interval was 1 cm)	32
Figure 17. Bed profile for $V_a/V_w = 85.65$. (Flow was from left to right. Contour interval was 1 cm)	32
Figure 18. Bed profile for $V_a/V_w = 99.92$. (Flow was from left to right. Contour interval was 1 cm)	33
Figure 19. Bed profile for $V_a/V_w = 114.20$. (Flow was from left to right. Contour interval was 1 cm)	33

Figure 20. Bed profile for $V_a/V_w = 142.75$. (Flow was from left to right. Contour interval was 1 cm)	34
Figure 21. Plain view bed profile photos from a through j resulting from varied air flow rate represented by ratio of air velocity to water flow velocity V_a/V_w (Flow was from left to right)	35
Figure 22. Side view of the flume with dye introduced at different positions for the base case ($V_a/V_w = 0$) (Flow from left to right)	37
Figure 23. Side view of the flume with dye introduced at different positions for $V_a/V_w = 71$ (Flow from left to right. Air diffuser hidden by bubbles.)	39

List of Tables

Table 1. Sediment size distribution and characteristics (Provided by Manufacturer: Red Flint Sand & Gravel, LLC. Eau Claire, Wisconsin)	15
Table 2. Parameters used in Experiments	20

Acknowledgements

I would like to thank my advisor, Dr. Brian Barkdoll for his guidance and encouragement throughout this project. I would like to extend my gratitude to Jennifer Tyrrell for her assistance in conducting experiments and data collection. I also want to thank Michigan Technological University for the research facilities and resources provided, which were a key part of this project.

I would like to thank my family for their ever present support. I am especially grateful for my mother, who continues to be a source of inspiration for me.

Abstract

Local scour is a major cause of concern for the stability of bridge piers and the safety of the public using the bridges. Structural countermeasures and flow-altering devices have been developed to deal with local scour. Many armoring structural countermeasures are very effective and efficient in clear water conditions but are susceptible to moving bed forms and leaching. The flow-altering devices are effective in both clear water conditions and moving bed forms, but are prone to clogging, less efficient in changing flow direction, etc. This study aims to reduce the local scour by injecting air in order to reduce the effect of the scour-inducing downward roller flow pattern by harnessing the buoyancy of the injected air bubbles.

A clear-water scour experimental study is conducted in a rectangular channel with a pier embedded in a sand bed. Air is injected through a horizontal diffuser pipe wound around the upstream half of the cylindrical bridge pier. Measurements were taken for maximum local scour depth, water surface profile, rate of scour, centerline scour elevation and channel bed profile at the equilibrium condition. The ratio of velocity of air to the velocity of water (V_a/V_w) was chosen as the non-dimensional variable for this study and was considered the most suitable representation and for ease of scalability. The air injection reduced the local scour at bridge piers in equilibrium conditions by nearly 35%. This scour reduction is caused by a change in flow patterns around the bridge piers with the injection of air bubbles. A dye test was performed for the base case (without air injection) and the optimal case ($V_a/V_w = 57.1$) to observe the change in flow behavior around the pier.

Chapter 1: Introduction

1.1. Introduction

Sediment scouring (scouring) is a natural phenomenon which washes away sediment around an obstruction caused by the formation of vortices in flowing water. Scour is a major cause of bridge failure in the United States (Harrison 1992). A large number of the bridges in use are old and were designed and constructed based on the conditions of rivers and riverbeds at the time of the project undertaking. Since rivers change as part of their natural geomorphology due to changes in the hydrology of the rivers and contributing watersheds, the safety of the bridge may be compromised by degradation of the riverbed over a long period of time, contraction scour, and local scour. This change presents a greater risk to the integrity of the bridge during extreme rainfall and flood events.

The design of bridges on waterways and channels with flowing water takes into consideration the relative scour and foundation depths. The existing formulas used to calculate the local scour are based on laboratory experiments and contain some level of uncertainty. This makes the scour countermeasures a must for bridges that exhibit excessive scour.

Over the years, studies have been done to improve the countermeasures by way of structural reinforcements to increase the shear strength of bed material by means of rip-rap, collars and other means. Flow alteration is also used to reduce the downward vortex and the downward shear stress exerted by the flow. The countermeasures are only effective if properly maintained. The cost, effort, and reliability involved with the design,

construction, inspection, and maintenance of countermeasures are a significant consideration in the selection of appropriate countermeasures.

Literature Review

Our knowledge of bridge scour and scour countermeasures has increased over the years and studies on countermeasures and other issues relevant to the present subject are presented below.

Bridge pier scour is dependent on a multitude of factors including depth of flow, flow velocity, pier shape and size, and minor factors such as water temperature, among others (Lagasse, et al. 2007). Bridge piers are protected by countermeasures using one of two approaches. One is to enhance the bed to increase its resistance to erosion, achieved by placing materials on the bed with higher critical velocities (armoring). The second approach is to reduce the erosive capacity of the flow, by re-directing downward flow away from the bed by means of collars and streamlining the piers to reduce the strength and size of the horseshoe vortex (flow altering) (Chiew 1992).

1.1.1. Existing Countermeasures

Riprap:

Rip-rap is the oldest and most widely-used countermeasure against scour. The equations for the sizing of riprap were derived by using boulders with critical velocity calculated by the formula given by (Isbash 1935). Koloseus (1984) concluded that riprap can have a tendency to magnify peizometric gradient at the bed of the channel, leading to increased leaching potential of fine sediment through the gaps in rip-rap (Koloseus

1984). Parola and Jones (1991) performed experiments on scale models to adjust the equations by a factor of 1.3 and 1.7 for circular and rectangular bridge piers. Riprap design is modified to include filters to prevent leaching of sediment beneath the riprap, caused by a difference in pressure between water on the bed and groundwater beneath the bed surface (Parola and Jones 1991).

Chiew and Lim (2000) conducted experiments to study the failure of riprap and identified that riprap can be very inefficient in flows with large dunes and ineffective as a scour countermeasure. A study by Lauchlan and Melville (2001) on riprap protection and failure modes agreed with that proposition and states that edge shear and winnowing mechanisms would play a secondary role leading to failure. Chiew (2004) stated that riprap stability is susceptible to bedform-induced failure, caused by live bed forms with large dunes resulting in riprap degradation. Channel bed degradation can result in formation of riprap mounds which are vulnerable to designed flood flow combined with large dunes, resulting in what is considered to be bed-degradation-induced failure.

Yoon (2005) produced a comprehensive study on the possibility of using wire gabions filled with riprap as an alternative to the loose riprap and concluded that wire gabions of similar size provide better protection compared to that of individual riprap. The study noted shear failure as the dominant cause of failure in the case of wire gabions. Yoon and Kim (2001) experimented on the use of sack gabions filled with riprap material as a countermeasure and concluded that the stability of a collective body of riprap scour countermeasures can reduce scour more than individual riprap. The study also noted increasing the length of sack gabions increased the critical velocity.

Bed Sills:

Chiew and Lim (2003) used a sacrificial sill as a pier scour countermeasure and found it to reduce the pier scour depth by 50% in its best configuration in clear water conditions. Grimaldi et al. (2009) investigated the use of bed sills just downstream of the pier as a scour countermeasure and found a reduction of 26% in the maximum local scour depth and a 80% reduction in scour area and volume when the sill was placed right downstream of the pier, contrary to the separation recommended by Chiew and Lim (2003). The study found that skewness in the flow can reduce the efficiency of the sill. Live bed conditions also reduce the efficiency to 20% scour depth reduction (Chiew and Lim 2003).

Collars:

Moncada-M, et al. (2009) experimented on the use of collars as a countermeasure against local scour at circular piers. This study found a total reduction of scour depth ranging from 55% to 96% for collars of diameter that are twice the diameter of the pier. The study also noted the scour depth reduced to zero with a collar of diameter that is thrice the diameter of the pier. The collars were most effective when they are placed at the bed level.

The collars were found to lose their effectiveness in live bed conditions and the trough of the migrating bed forms were found to expose the pier beneath the collar (Chiew 1992).

Slots:

Chiew (1992) used slots in the pier to reduce the scour at the base of the piers. This is to reduce the downflow created by the horseshoe vortex from impinging on the bed or to divert the downflow away from the bed. The study noted that slots placed near the bed are effective in reducing the scour by 20%. A slot used in conjunction with the collar can eliminate the scour altogether in clearwater conditions. However, the vulnerability of collars in live bed conditions might be an important factor in regards to the reliability of the combined system.

Grimaldi et al. (2009) used slots and achieved a scour reduction of 30% in clearwater conditions. A combined system of a slot and sill was able to reduce the scour depth in front of the scour by 49% in the best case and 45% on average. This combined system also reduced the area and volume of the scour by 85.5% and 92.3%, respectively, which could be useful in reducing the overall scour resulting from the presence of the pier. This study concluded that a slot was an effective countermeasure against scour from the beginning of the test and would be suitable for control of scour over the long term, as well as the short term. Debris allocation and a skewed alignment of the slot with respect to water can reduce the effectiveness of the slot as a countermeasure.

Sacrificial Piles:

Sacrificial piles are piles placed upstream of the bridge pier to deflect the high velocity flow away from the bridge piers. These piles absorb energy from the flow that would otherwise cause pier scour. A triangular configuration was tried by Melville and

Hadfield (1999), who found that the effectiveness of these piles are dependent on approach angle, flow intensity, geometric arrangement, spatial arrangement and size with respect to the piers and protrusion of the piles which makes the design and thereby the effectiveness as a countermeasure very uncertain and unreliable in meandering channels and during floods. A triangular configuration with the apex pointed upstream is considered to be the most effective. Sacrificial piers are found to be effective in clearwater scour conditions. However, these piles are also found to be susceptible to dune migration downstream. The study also found that the piles are ineffective as a countermeasure against scour in live bed conditions if the approach angle is $> 20^\circ$.

Vanes:

Vanes are used to redistribute the flow in channels and used as countermeasures to bridge scour when designed to divert the flow away from the bridge piers. Experiments conducted by Tafarjnoruz, et al. (2012) showed that the scour depth reduction efficiency at equilibrium for submerged double vanes placed at short distances from the pier is at a meager 12.4% in contrast to the results reported earlier. This difference is largely attributed to the duration of the experiments and experimental set up. This study also noted that vanes may partially prevent scour by entrapping the sediment, but as the scour deepens around the vanes, the vanes divert a higher portion of flow on to the face of the pier, thereby increasing the scour potential.

1.1.2. Bubble Screen

Dugue et al. (2015) studied the effects of an air bubble screen and its effect on recirculating water and its effect on bed morphology. The strength and size of the

secondary flow field was analyzed in three different experimental conditions of still water, flow on an immobile sand bed, and flow on a mobile sand bed with sediment transport. The experiments revealed that the strength of the secondary cell increased with water depth and had no significant influence on the base flow. The secondary flow influenced the longitudinal velocities by adjective redistribution that led to morphological redistribution. The experiments were conducted using air jets angled upward and do not directly relate to the present study, but the principle of using air bubbles to redistribute the velocity and sediment is related to the principle of present study. This study stated that the rising air bubbles have the potential to counteract the downward flow which lead to the local scour at the bridge piers.

Champagne et al. (2016) conducted comprehensive studies to reduce local scour downstream of a spillway-stilling basin structure. Air was injected through an air diffuser downstream of the stilling basin. The study examined the effects of different parameters such as approach flow, tailwater conditions, bed sediemnt, and air injection discharge to determine the optimal configuration for maximum reduction in local scour. The air injection configuration was varied with respect to the flow rate which in turn was represented as air-water velocity ratio, injection angle, air holes spacing, and air-hole diameter. An optimal scour reduction of 37% away from the structure and 57% near the structure was observed. The optimum configuration was achieved when the air injection was angled perpendicular to the flow. Although the flow regime is completely differenc from that around a bridge pier, this study is paticularly important and significant in the context of the present study as this was the only study that documented the effect of air injection on local scour.

Existing countermeasures for bridge scour listed above in the Literature Review section are vulnerable to bed forms or their effectiveness is reduced in live bed conditions by debris accumulation (a major concern during floods and skewness of flow, which is a factor to be considered in natural meandering channels).

The structural countermeasures are designed to minimize or in some cases eliminate local scour altogether. This could have an effect on the aquatic life as some fish would prefer pools. The presence of scour holes would enhance the habitat for the fish, but can be hazardous for the structures in the stream (Barkdoll and Huckins 2012). This study is aimed at reducing the bridge scour (local scour) in such a way that it does not prevent the scour but allow it to a level that prevents bridge collapse and minimizes the adverse effects emanating from the presence of the pier.

1.2. Objective

The objective of this study is to experimentally investigate the use of air injection as a countermeasure against local scour. Its effectiveness as a countermeasure is investigated as an alternative to the existing countermeasures which are constrained by reliability, effectiveness, efficiency in different flow conditions, and ecological impact. Experiments are conducted to examine the applicability of air-injection as a countermeasure for bridge scour.

Specific goals of this study include:

1. Determine if air injection can reduce bridge scour
2. Determine the optimum air injection flow rate for maximum scour reduction

Chapter 2: Procedure

2.1. Experimental Set up

2.1.1. Laboratory

The experiments for the present study were carried out in the hydromechanics laboratory located in the Dillman Hall 110 at Michigan Technological University.

2.1.2. Flume Setup

Flume Features:

The masonry block flume in the laboratory consists of an inlet section, flow developing section, scour basin, sediment trap, and outlet section (in order from upstream to downstream). A picture and a schema of the flume are presented below in **Figure 1** and **Figure 2** respectively. The flume is 10.18 m (33.39 ft.) long, 0.92 m (3.00 ft.) wide on the inside, and 1.04 m (3.41 ft.) tall. The outer wall of the flume was constructed using concrete blocks on a concrete slab floor. The inside of the walls were lined with a water sealant to prevent leakage. There are two wooden inner walls separating the head tank, the main channel and the sediment trap section. The flow straightening section has small PVC pipes parallel to the flume. The base of the flow developing section was constructed using wood. A PVC pipe was used to simulate a pier located in the sediment scour testing section.

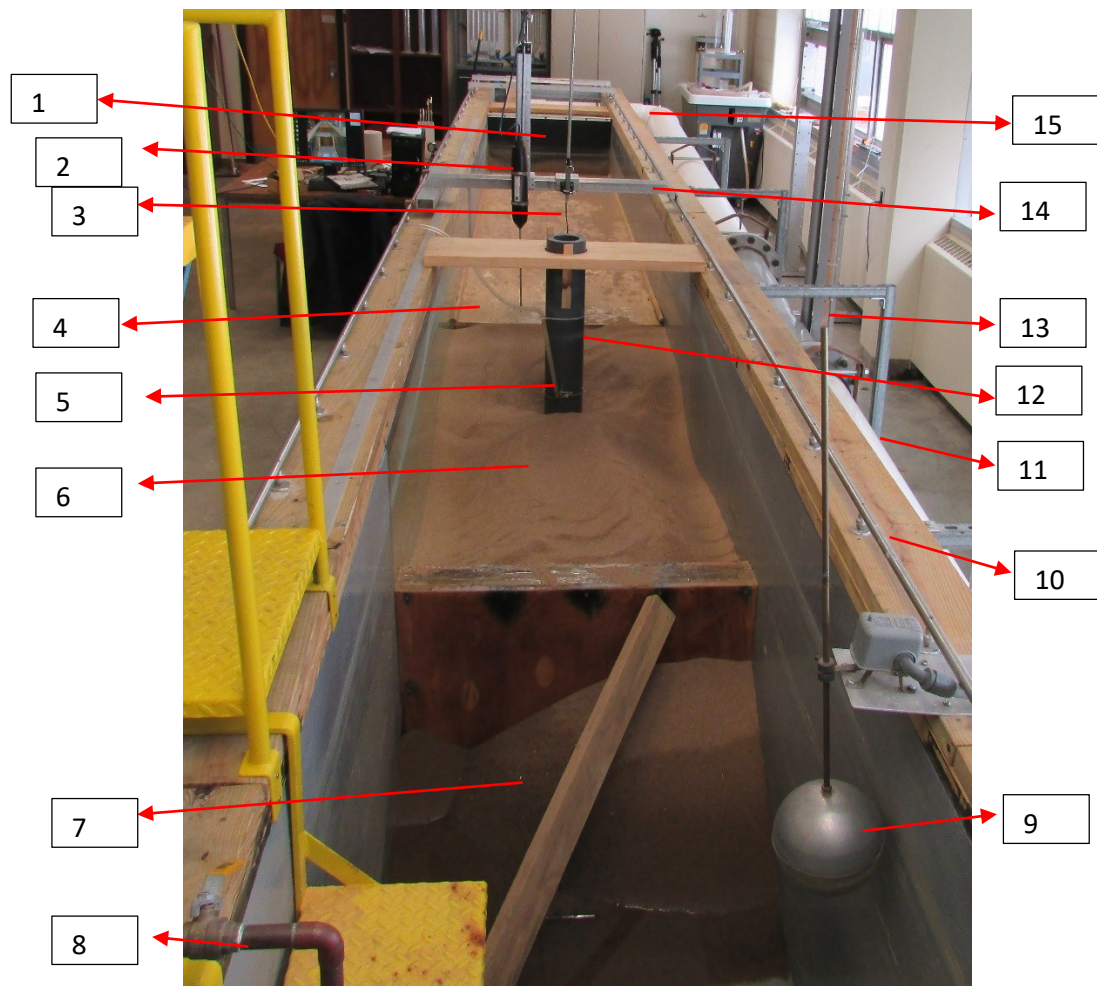


Figure 1. View of flume looking upstream. Features are described in the numbered list below

1. Flow levelling rubber mat
2. ADV
3. Point gage
4. Flow developing section
5. Air supply

6. Scour section
7. Sediment trap
8. Water Supply
9. Float valve
10. Guide rails
11. Recirculating pipe
12. Pier
13. Monometer
14. Instrument carriage
15. Inlet pipe

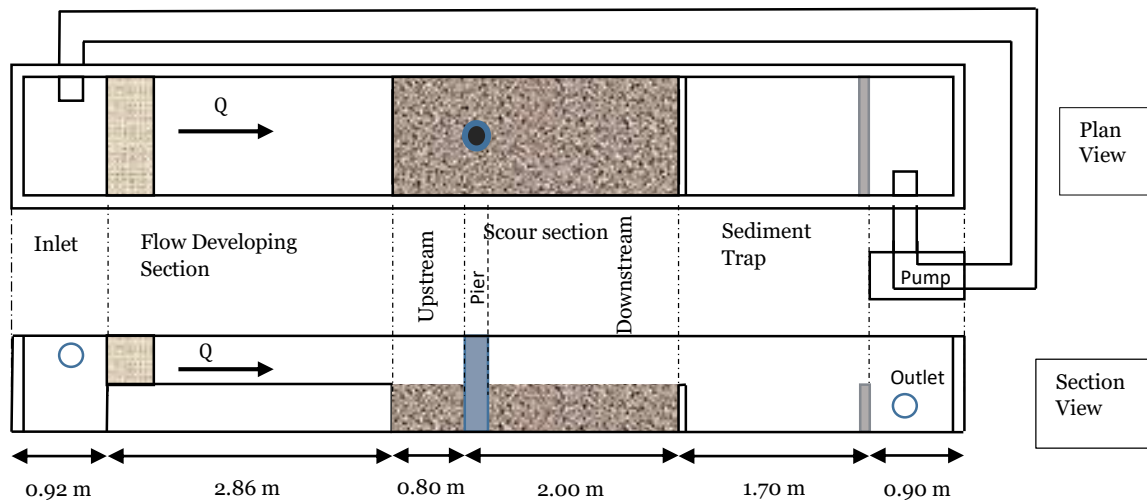


Figure 2. Schema of flume with sections

The inlet section is 0.915 m long and has an inlet pipe of diameter 0.254 m (10 in.) with 3 elliptical cuts on the downward facing side to allow water to exit. This directs the incoming flow downward, thereby minimizing the disturbance in water level created

by the incoming concentrated flow. The inlet section is separated from the flow-developing section by a wooden wall that is 0.66 m (2.17 ft.) high. Above the wooden wall is an array of PVC pipes 20 mm (0.82 in.) in diameter, stacked parallel to each other and parallel to the channel to straighten the flow that enters the flow developing section.

Water enters the flow developing section with a wooden floor, passing through a rectangular rubber mat installed to level the water surface. This ensures the flatness of water surface across the channel cross-section. Downstream of the flow developing channel was the 2.805 m (9.20 ft.) long scour basin filled to the same level as the fixed bed with sand with $d_{50} = 0.56$ mm. The size distribution of the sediment is shown in the **Table 1***Error! Reference source not found.*. The bottom boundary of the scour section was the existing concrete flooring. A circular pier made of thick PVC pipe with an outer diameter of 14.2 cm (5.6 in.) was placed on the centerline at a distance of 0.8 m downstream of flow developing channel. The ratio of width of the flume to the diameter of the pier was calculated to be 6.47, providing enough room for the flow to be free of interference from the side walls. The pier is secured firmly with the help of a wooden plank fixed to the top of the flume, reinforced to resist disturbances created by flowing water and injected air. The pier has a uniform cross section and was aligned perfectly vertical. The scour section ends with a wooden wall fixed in place, reinforced with a wooden bar against a concrete partition at the end of sediment trap.

A sediment trap section with a length of 1.70 m (5.58 ft.) was constructed just downstream of the scour section. This section trapped the sediment and prevented sediment recirculation, reducing the internal wear of the pump due to the abrasive nature of the sediment.

Water then entered an outlet section 0.9 m (2.9 ft.) in length. This section housed an outflow pipe 0.254 m (10 in.) in diameter that fed a centrifugal pump to recirculate the flow to the upstream of the flume (inlet section). The air injected in the scour section dissipated before reaching this section and so did not have an effect on the pump operation. The bubbles generated in the inlet section due to the downward directed inflow from the recirculating pipe surfaced as they passed through the flow straightening section.

The water level in the flume was kept constant by an adjustable float valve located in the sediment trap section as seen in **Figure 1** (Component No. 9). This float was attached to an adjustable rod connected to an electronic valve which controls the water feed to the flume from the city water supply. This accounted for minor losses of water due to evaporation and any minor leaks during the course of the experiments. This maintained constant water levels throughout experiments with an accuracy of ± 3 mm. The water feed pipe was installed with surge protectors to minimize the effects of water hammer generated by sudden closing of the valve.

Compressed air used in the experiments was routed using a combination of 2.5 cm (1 in.) diameter steel piping and 1.905 cm (0.75 in.) transparent rubber pipe. The air was then routed through a steel diffuser pipe with an inside diameter of 4.2 mm (0.165 in.) and outer diameter of 6.6 mm (0.26 in.). The diffuser tube was installed at the same elevation as that of the flow developing section and the initial bed elevation where it was wound horizontally around the upstream half of the pier as shown in **Figure 3**.



Figure 3. Steel diffuser pipe around the upstream half of the pier (looking downstream)

This diffuser pipe had 24 holes drilled in it pointing horizontally radially outward and approximately cover 180° in the upstream face of the pier. The diameter of the holes were 1.65 mm (0.065 in), which remained constant for all the experiments. Two different gages were used during the experiments to monitor the air flow rate and air pressure. The air flow gage had a least count of 0.00047 cms (1 cfm) and was then recalibrated to a least count of 0.00024 cms (0.5 cfm) by linear interpolation. The air pressure gage was installed downstream of the air flow gage with least count of 6.9 k.Pa (1 psi), but air flow rate was used for monitoring air injection condition and not air pressure.

Water was recirculated in the flume by means of a centrifugal pump with variable-speed equipped with electronic controls. The pump input was in terms of impeller frequency, with a least count of 0.01 Hz. The water flow rate was measured using a two-tube monometer at the contraction, constructed from a 1.829 m (72 in.) long stainless steel pipe section in the recirculating pipe with the same diameter. The monometer measured the pressure difference on both sides of the contraction. The monometer had a least count of 0.0037 cm (0.01 ft.). This would result in a flow rate accuracy of $\pm 0.0058 \text{ m}^3/\text{s}$ ($0.204 \text{ ft}^3/\text{s}$).

An instrument carriage is placed to host instruments for data collection. This was constructed from an aluminum C section and was equipped to slides on rails which run along the length of the flume. These rails were laser levelled to an accuracy of $\pm 0.035 \text{ mm}$ (0.001in.). The instruments were mounted using friction fit.

Table 1. Sediment size distribution and characteristics (Provided by Manufacturer: Red Flint Sand & Gravel, LLC. Eau Claire, Wisconsin)

COEFFICIENT	VALUE
$D_{85} =$	0.6949 mm
$D_{60} =$	0.5927 mm
$D_{50} =$	0.5557 mm
$D_{30} =$	0.4884 mm
$D_{15} =$	0.4439 mm
$D_{10} =$	0.4266 mm
$C_U =$	1.39 mm
$CC =$	0.94 mm

2.2. Experimental Procedure

The following procedure was followed for conducting all the experimental runs.

1. Level the sediment in the scour section of the flume to the top of the flow developing section and the top of partition wall with sediment trap section
2. Fill the flume to the desired flow depth (same for all experiments)
3. Start the flow, slowly increasing the flow to the desired flow rate (same for all experiments)
4. Start the air flow, slowly increasing to the desired flow rate
5. Measure the depth of scour hole at the face of the pier facing upstream until equilibrium
6. Measure water surface profile
7. Stop the flow, slowly reducing the pump impeller frequency to zero
8. Drain water
9. Measure bed profile elevation

2.3. Data Collection

A point gage was used for collecting scour, water, and bed surface profiles. This gage was mounted on the instrument carriage. The point gage has a least count of 0.1 mm (0.04 in.). The elevation of the center of the fixed bed at the end of the flow developing section was used as a reference in calculating the depth of scour. Since as the scour hole deepened the rate of scour reduced, scour measurements were taken at intervals of 5-10 mins at the start of the experiments and the intervals increased as the experiment progressed.

A thermometer was used in collecting the water temperature data in an effort to document any temperature differences, such as those induced by pump. The thermometer had a least count of 1° C. But, the temperature data was not used in any analysis during the course of this study.

A Sony CyberShot W120 digital camera was used to record video and take pictures of the scour process. Photos were taken of the bed profile in the upstream and downstream sections in order to understand the changes in bed morphology caused by different levels of air injection. The air injection interface was recorded on a video for a short duration of time, intended to replicate laboratory observations.

A Nortek Vectrino+ Velocimeter (Acoustic Doppler Velocimeter or ADV) manufactured by Nortek AS was used to collect depth measurements at the scour hole at the face of the pier. This was employed in only one experimental run without air to observe the effect of bed movement on the time evolution of scour. The air entrained in the water in close proximity to the pier was considered to disrupt the sound signals and interfere in the depth measurement collection, and so was not used in any other cases where air injection was used. The ADV was mounted on the instrument carriage and was aligned with the help of spirit levels.

2.4. Experiments

2.4.1. Scour Experiments

The experiments in the present study were carried out to determine if the air injection was effective as a countermeasure against bridge scour. First, an experiment

was conducted without air that served as a benchmark for further experiments with varied air flow rate. This is referred to as the base case throughout the course of this study. Further experiments were carried out with air flow rate varying from 0-17 m³/h (0-10 cfm). The increments were of 0.85 m³/h (0.5 cfm) and 1.7 m³/h (1 cfm). The variations were determined based on the results presented in the next chapter to better understand the behavioral changes and sensitivity of air flow on the scour and bed morphology.

The ratio of velocity of air (V_{air}) calculated as the (air flow rate)/ (total area of diffuser holes) and velocity of water (V_{water}) calculated as the (approaching water flow rate)/ (cross sectional area of the approaching water flow) V_{air}/V_{water} or (V_a/V_w) was the non-dimensional parameter varied throughout the study and its effect on maximum scour depth was documented. V_a incorporates the air flow parameters such as air flow rate, diameter of the holes, and number of holes in the air diffuser pipe. V_w incorporates various water and channel parameters such as water flow rate, channel width, slope of the channel, Manning's roughness coefficient, and depth of water flow. Since the velocity ratio incorporates such a wide range of parameters, V_a/V_w was chosen as the most appropriate representation of the configuration in terms of scalability. The level of flow disturbance caused by the air injection was also documented through water surface profiles along the centerline by measuring the elevations of crests and troughs of the waves. The bed profile was measured using the point gage on a 10 cm X 10 cm grid. The bed elevation was measured at the node of each grid and bed contour plots prepared using MATLAB.

The experiments were conducted by varying air flow rates while keeping the water flow rate constant for all experiments at a value just below visually-confirmed

incipient motion. Clear-water scour conditions were used since they result in the deepest scour without having bed sediment movement filling in the scour hole and, thereby reducing scour. Some runs were repeated to test the repeatability of the study and the results. The scour hole deepens as the sediment is transported by the flowing water and reaches equilibrium when the amount of sediment transported away from scour hole by water flow equals the amount of sediment filling the scour hole under the effect of gravity. In the present study the experiments were run until it attained equilibrium. The criteria for scour equilibrium was: scour of less than 0.5 percent change over 2 hours. Due to the nature of the rate of scour and the limitations of data collection, this translated to scour of less than 0.1 mm (minimum detectable) over 2 hours.

Table 2. Parameters used in Experiments¹

S. No.	Q _{air} , cfm	Q _{air} , m ³ /h	Average air velocity (V _{air}), m/s	V _{air} / V _{water} (V _a /V _w)	No. of Repetitions
1	0	0	0	0	5
2	0.5	0.85	2.3	7.14	1
3	1.5	2.55	6.89	21.41	1
4	2.5	4.25	11.49	35.69	1
5	3.5	5.95	16.09	49.96	2
6	4.0	6.80	18.39	57.10	1
7	4.5	7.65	20.69	64.24	1
8	5.0	8.50	22.90	71.37	5
9	5.5	9.35	25.20	78.52	1
10	6.0	10.20	27.59	85.65	2
11	7.0	11.90	32.19	99.92	1
12	8.0	13.60	36.79	114.20	1
13	9.0	15.30	41.38	128.79	1
14	10.0	17.00	45.98	142.75	1

¹ Water flow was constant for all the experiments with Q_w = 0.0606 m³/s and V_w = 0.322 m/s

2.4.2. Dye Test

A dye test was conducted for the base case (no air) and the optimal case ($V_a/V_w = 71.37$) to observe the change in flow behavior near the pier. Colored dye was introduced into the flow at the upstream face of the pier in the equilibrium condition at different positions along the height of the pier and the results are documented through photographs. The dye was injected using a long needle and care was taken to minimize the disturbance to the flow during this process.

Chapter 3: Results

The results are divided into six sections.

1. Rate of scour
2. Equilibrium Scour Depth
3. Centerline Scour Depth
4. Time to equilibrium
5. Water surface profile
6. Bed profile
7. Dye test

3.1. Rate of Scour:

The rate of scour was obtained by plotting the scour depth measurements in chronological order from the start of an experimental run until scour equilibrium was obtained. Scour equilibrium was defined as less than a 0.5 % change in 2 hours. **Figure 4** below shows the variation in rate of scour for different velocity ratios and at different point of time during the course of an experiment.

In the initial stages of the experiments, higher velocity ratio (higher air flow rate) results in increased rate of scour as can be observed from the slopes of each curve in the graph (**Figure 4**). This might be due to the direct interaction between the air and the bed during the initial stages as the air diffuser is at the initial bed elevation.

As the experiments progress and the scour hole deepens, the rate of scour trend reverses and the cases with higher velocity ratio (higher air flow rate) have a lower rate of

scour at a given point of time compared to the cases with lower velocity ratio (lower air flow rate). This is due to the progression of the experiments towards the equilibrium. In the cases with higher velocity ratio, the experiments are closer to equilibrium than that of a case with lower velocity ratio at a given point of time and the rate of scour reduces as the experiments progress toward equilibrium.

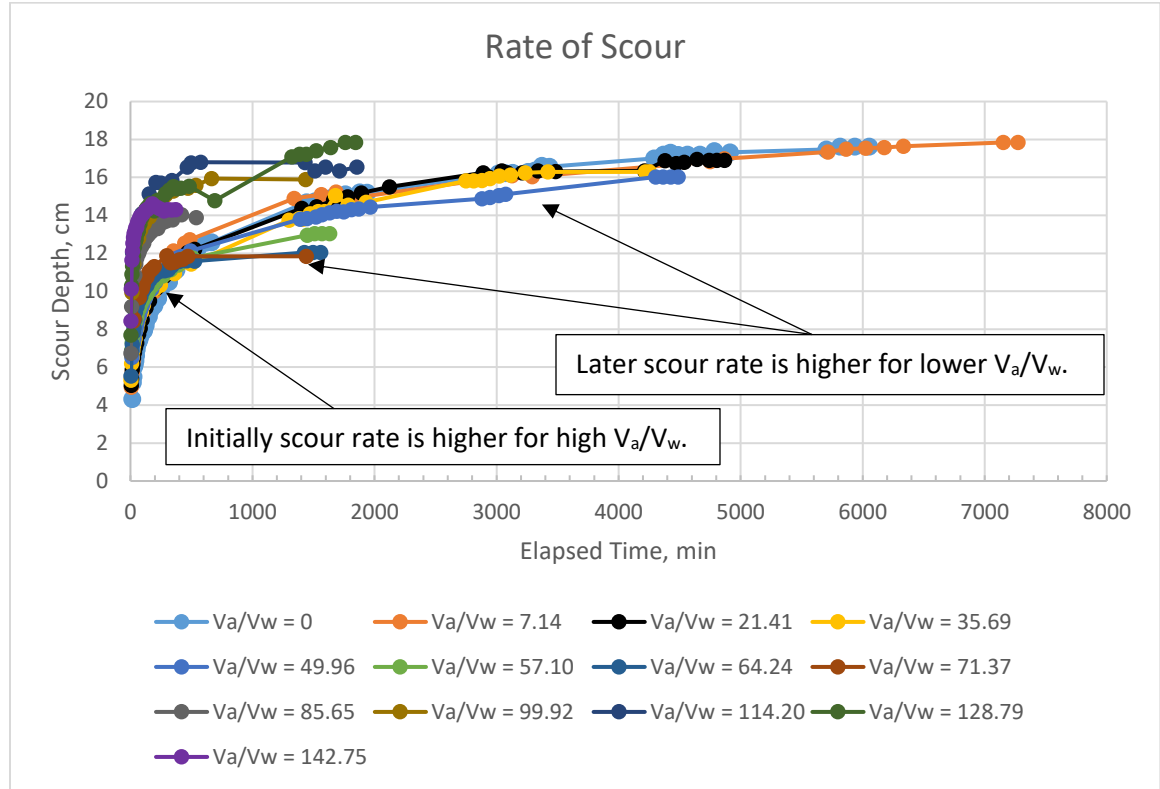


Figure 4. Rate of scour with varied air flow rate

3.2. Equilibrium Scour Depth

The depth of scour is the maximum depth measured at the upstream face of the pier in equilibrium condition. The results are plotted with V_{air}/V_{water} on the x axis and d_s/d_{s0} where d_s is the equilibrium scour depth for a specific air flow rate and d_{s0} is the

maximum depth of scour for the base case without air flow (**Figure 5**). This gives an accurate representation of change in scour depth as a percentage of the base case scour value. The error bars represent the mean \pm one standard deviation for the cases which were repeated. The hollow data points represents the results obtained in the first run of the repeated cases and may, therefore, not be as accurate due to experimental procedures still being perfected. It can be seen that the V_a/V_w value that results in the least scour is 57.1 that results in a reduction of $100(1-0.67)/1 = 33\%$.

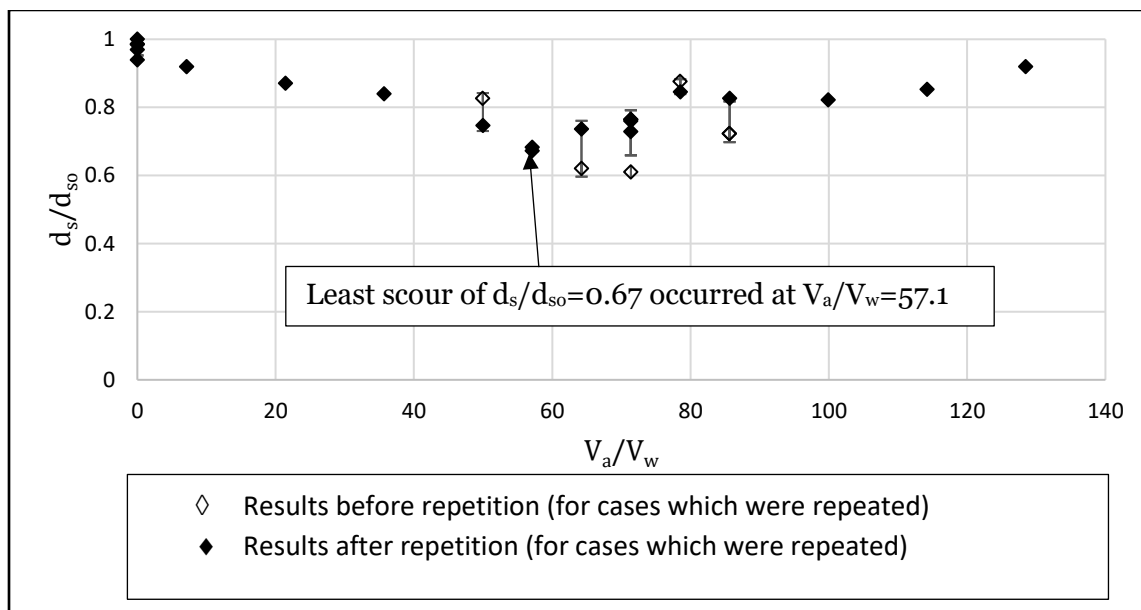


Figure 5. Scour depth variation with change in air flow rate

3.3. Centerline Scour Depth

The centerline scour depth is derived from the bed profile data collected after each experiment. The scour depth at $X= 0$ and $X= 20$ is averaged to obtain the scour depth at $X= 10$, which is inside the pier. **Figure 6** represents the change in

centerline elevation with respect to the initial bed elevation. It can be observed that the deepest scour is attributed to the base case with no air. It can also be observed that the pattern of the scour downstream of the pier in the case of high air flow ($V_a/V_w > 71.37$) deviates from that of low air flow and no air. In these high air flow cases, the scour downstream of the pier increased.

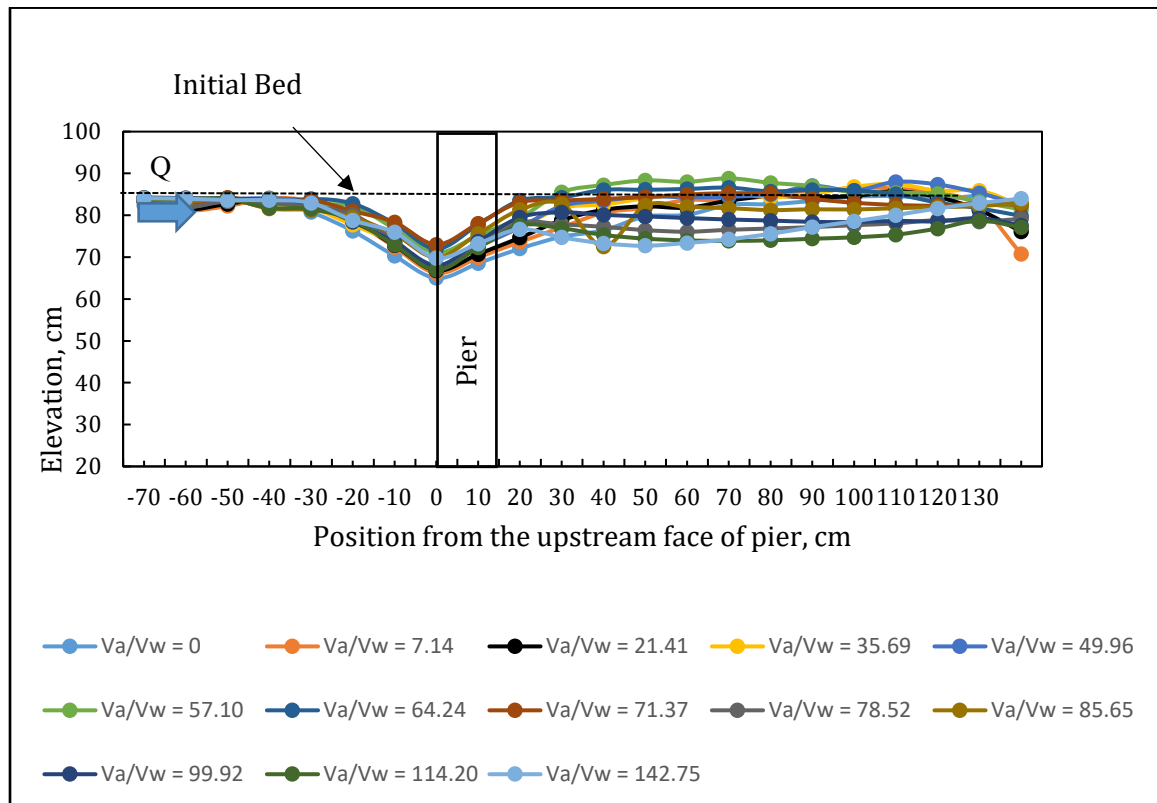


Figure 6. Centerline bed elevation with varied air flow rate

3.4. Time to Equilibrium

The time elapsed from the start of the experiment to the first time the equilibrium depth was encountered is represented as the time to equilibrium (**Figure 7**). Due to experimental data collection difficulties, there is some scatter in the scour equilibrium time values.

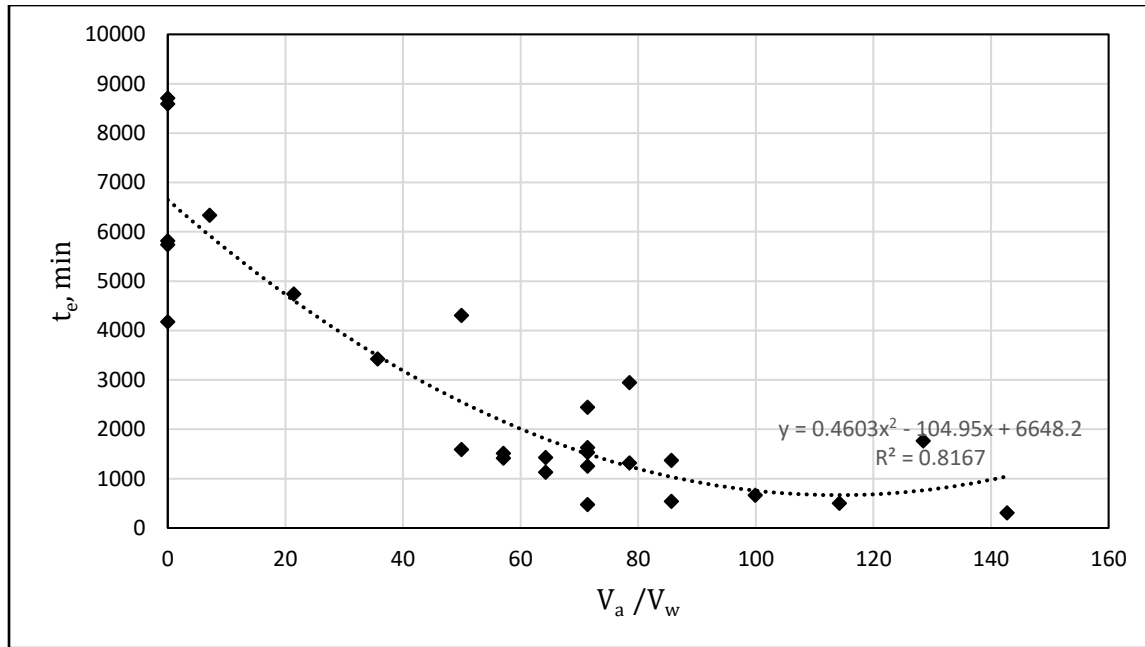


Figure 7. Time to equilibrium with varied air flow rate

3.5. Water Surface Profile

The water surface profile is obtained by measuring the water surface elevation using a point gage. The water surface exhibited some air-induced waves caused by air bubbles rising to the surface (**Figure 8**). The elevation of crest and trough were used, therefore, to derive the average water surface elevation.

The X-axis represents the position along the channel length from the upstream face of the pier where the maximum water surface elevation occurred.

The water surface elevation is not measured just behind the pier due to obstruction of the point gage instrument, except for the base case with no air flow ($V_a/V_w = 0$) and the case with $V_a/V_w = 71.37$, as the measurements were made at nodes of the 10 cm x 10 cm grid cells.

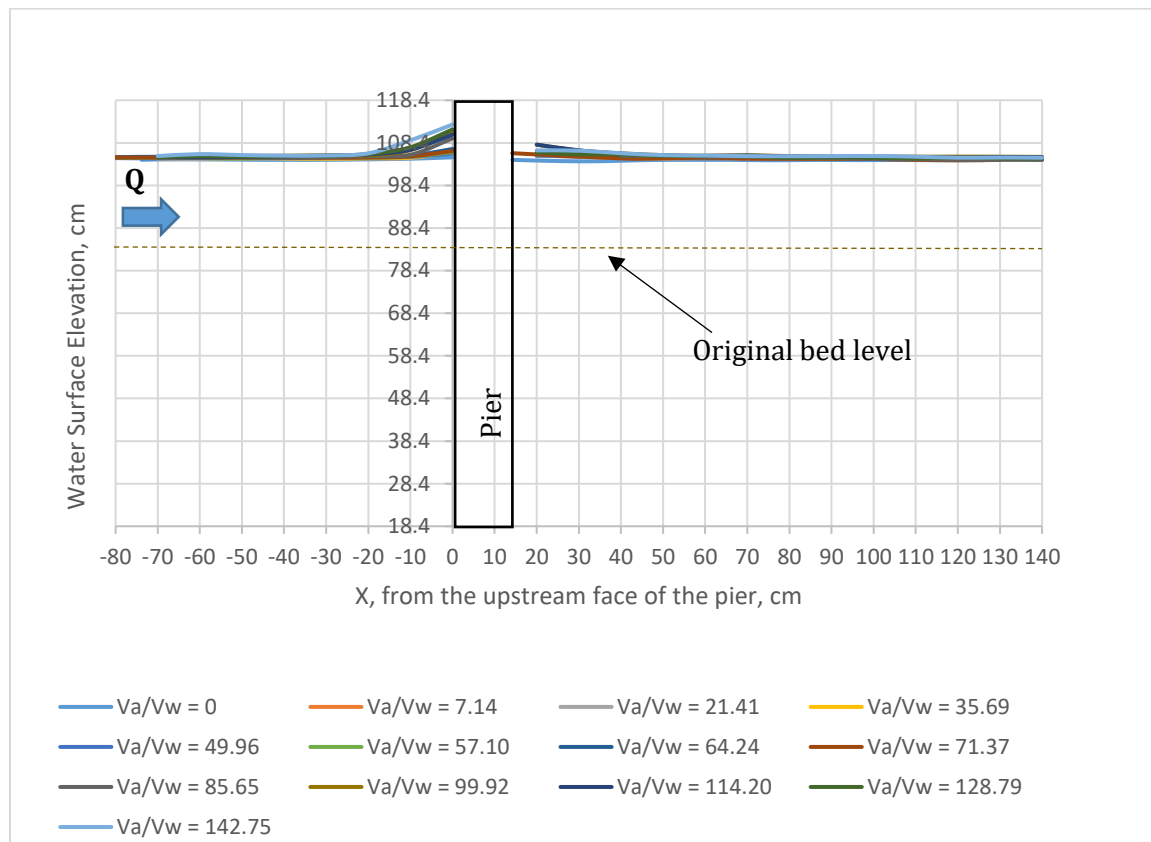


Figure 8. Water surface elevation with varied air flow rate

3.6. Bed Profile

The bed profile was measured using the point gage on a 10 cm x 10 cm grid from the point of deepest scour at the upstream face of the pier. These data points are plotted to form a contour for each case in **Figure 9** through **Figure 20**.

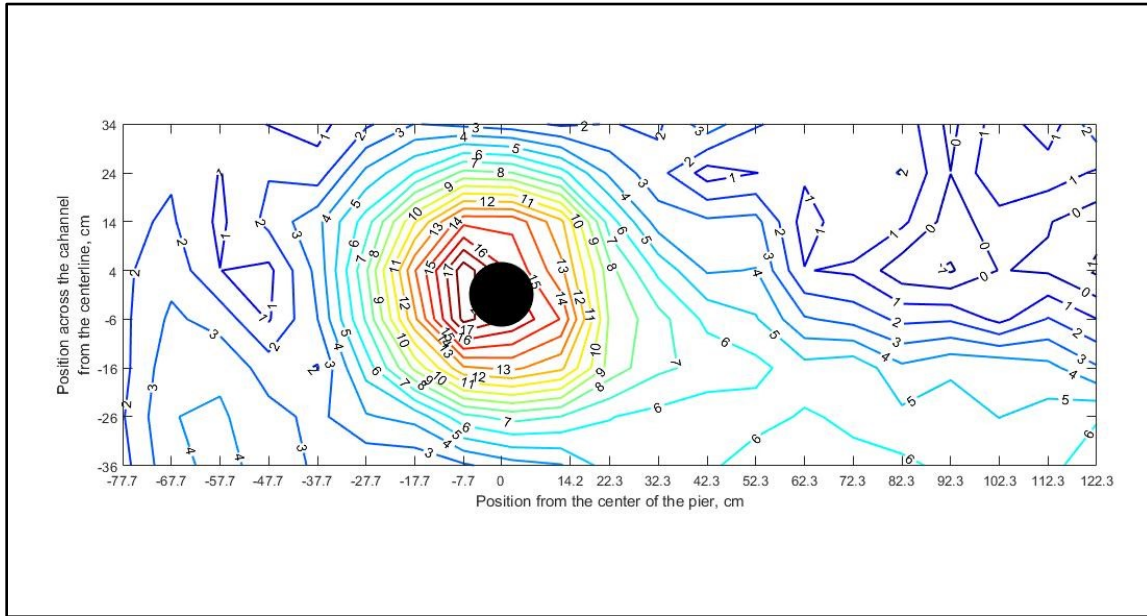


Figure 9. Bed Profile for the base case of $V_a/V_w = 0$. (Flow was from left to right. Contour interval was 1 cm)

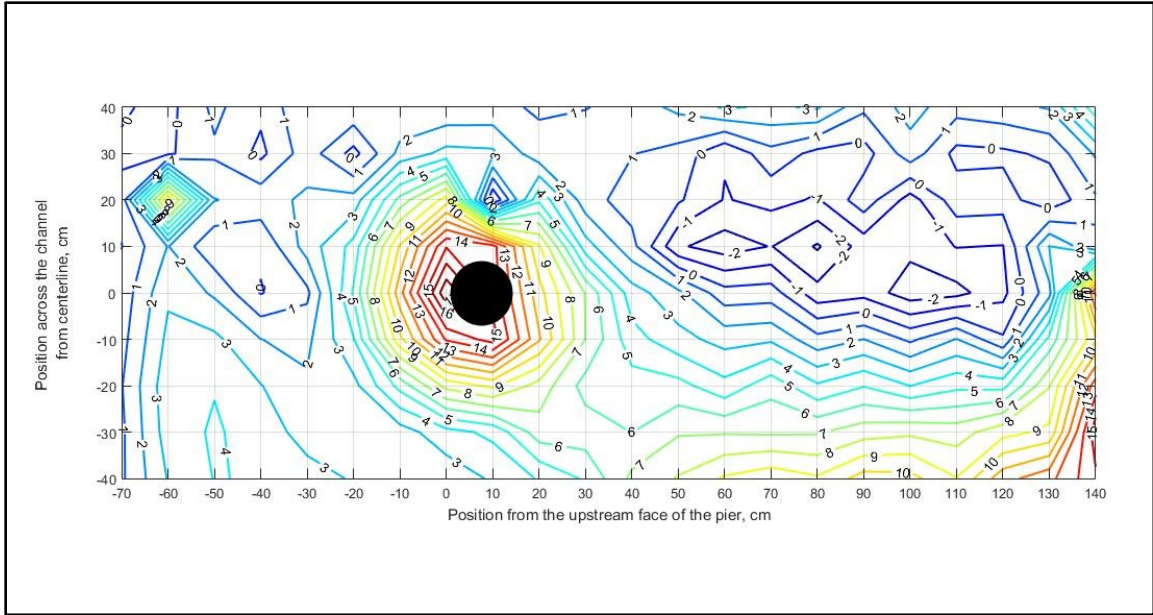


Figure 10. Bed profile for $V_a/V_w = 7.14$. (Flow was from left to right. Contour interval was 1 cm)

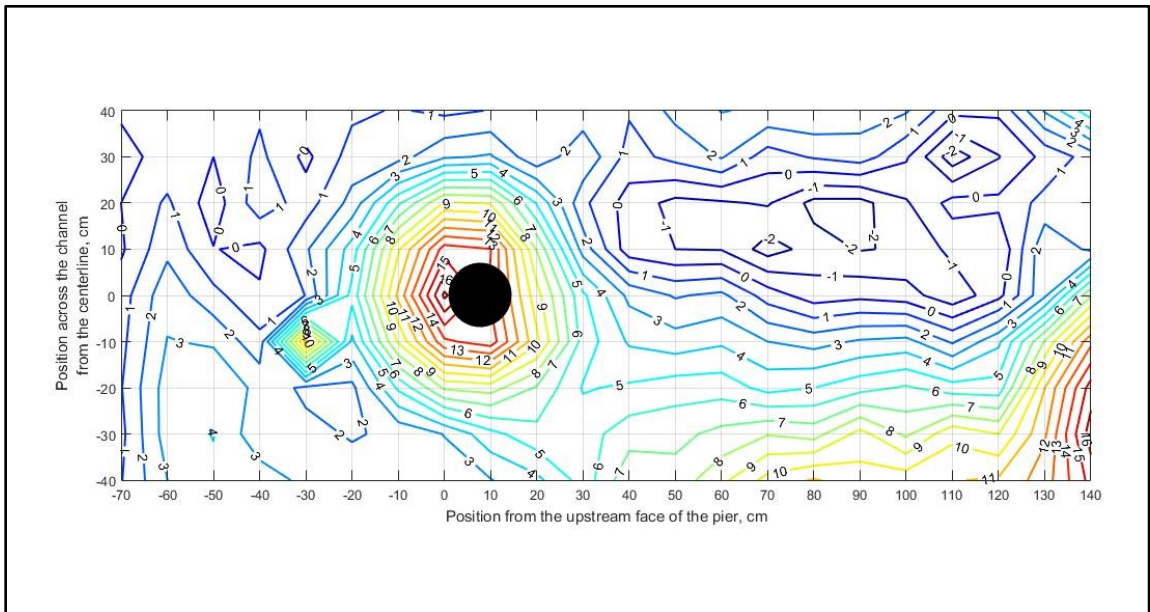


Figure 11. Bed profile for $V_a/V_w = 21.41$. (Flow was from left to right. Contour interval was 1 cm)

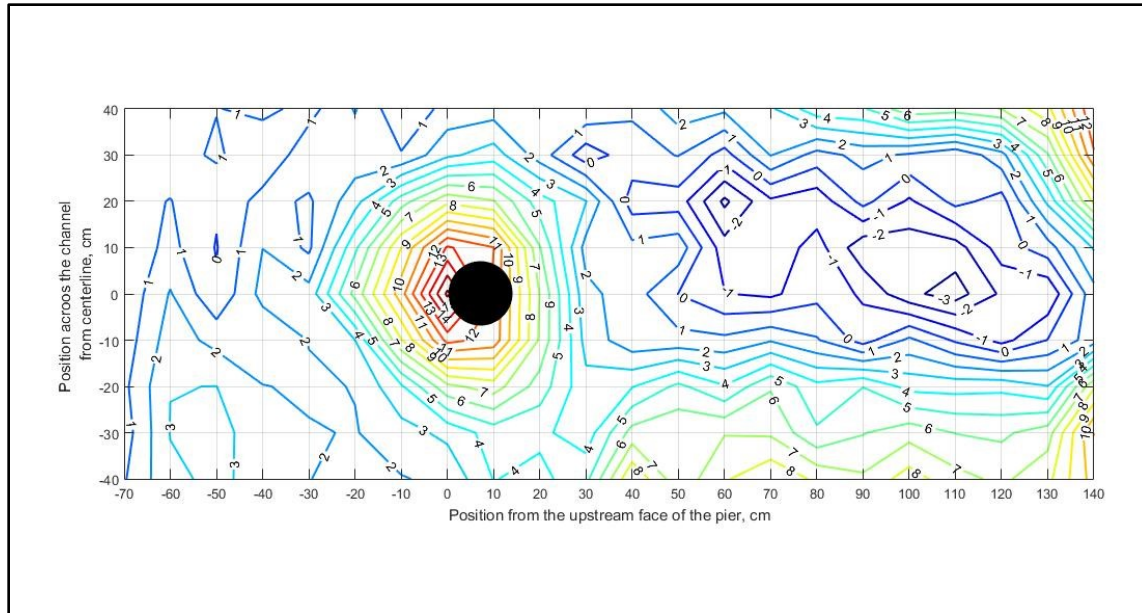


Figure 12. Bed profile for $V_a/V_w = 35.69$. (Flow was from left to right. Contour interval was 1 cm)

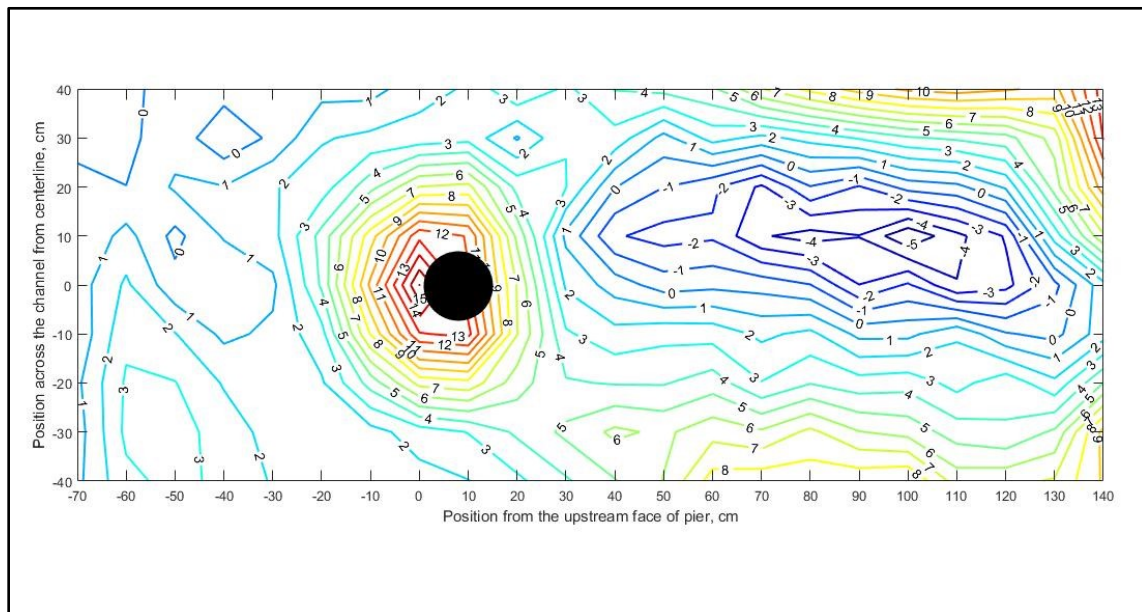


Figure 13. Bed profile for $V_a/V_w = 49.96$. (Flow was from left to right. Contour interval was 1 cm)

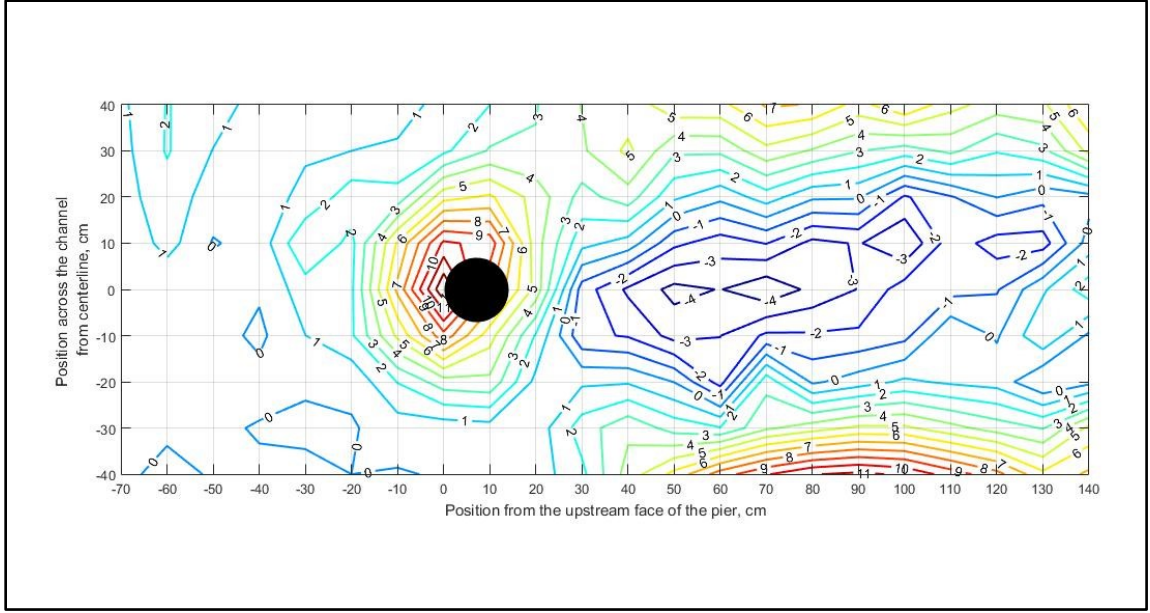


Figure 14. Bed profile for $V_a/V_w = 57.10$. (Flow was from left to right. Contour interval was 1 cm)

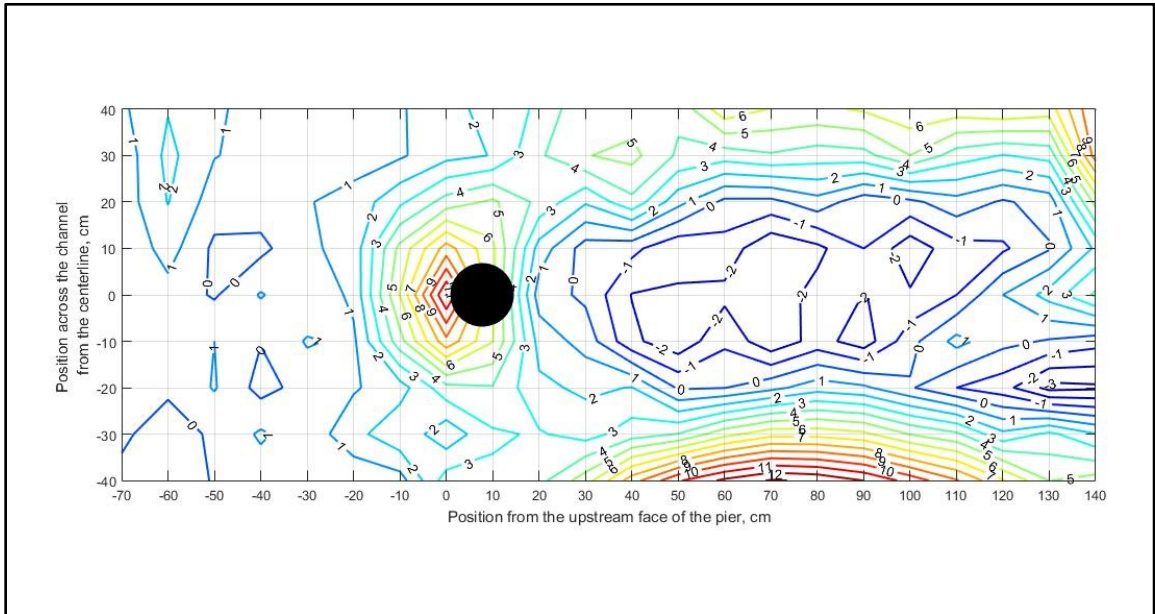


Figure 15. Bed profile for $V_a/V_w = 64.24$. (Flow was from left to right. Contour interval was 1 cm)

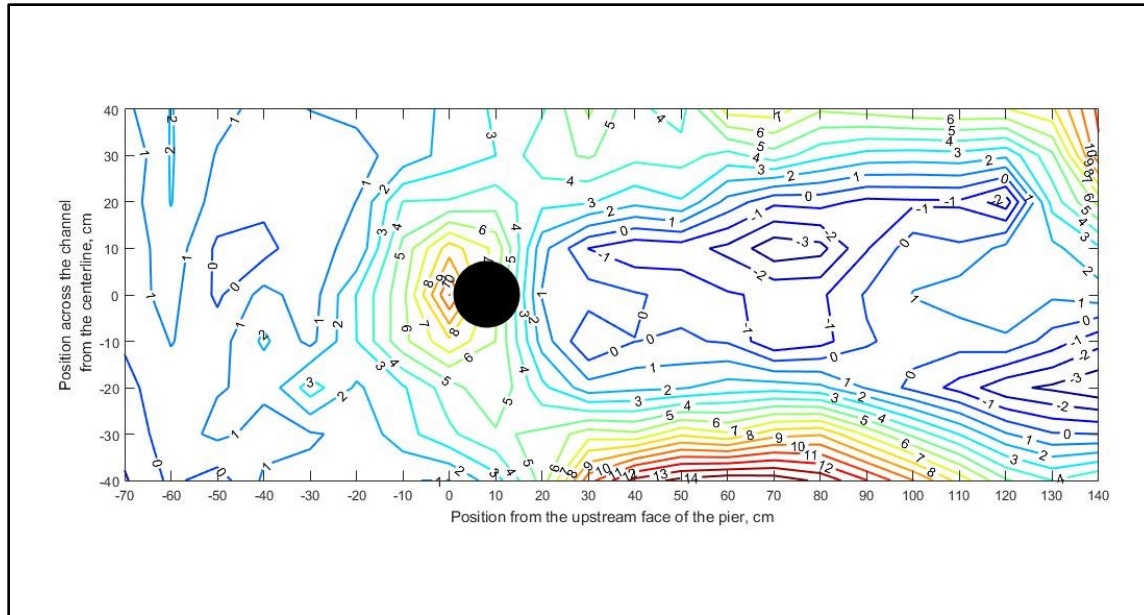


Figure 16. Bed profile for $V_a/V_w = 71.37$. (Flow was from left to right. Contour interval was 1 cm)

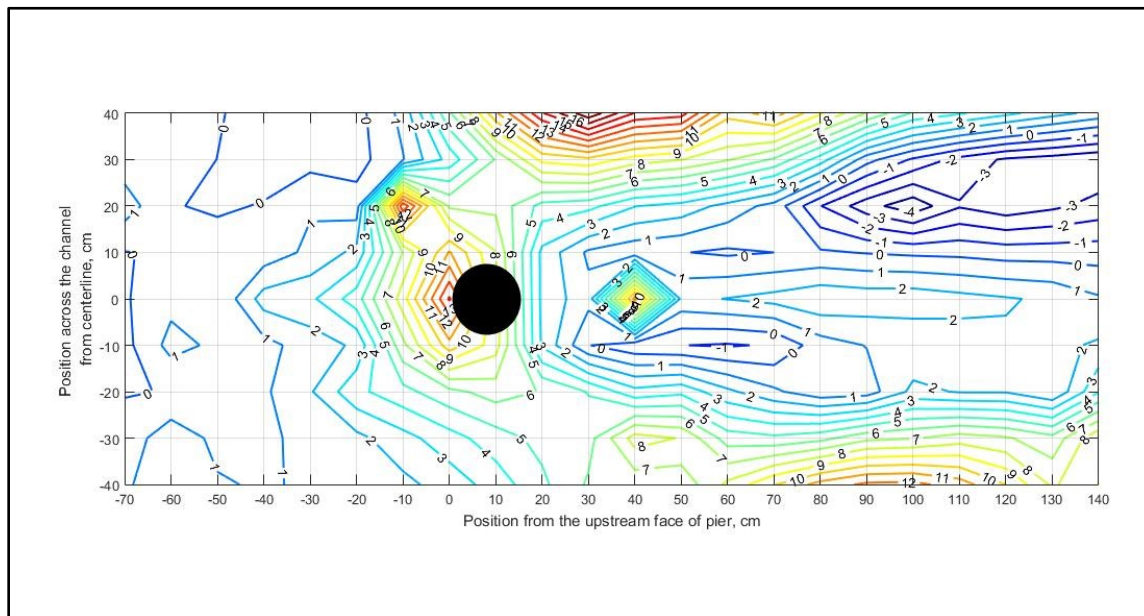


Figure 17. Bed profile for $V_a/V_w = 85.65$. (Flow was from left to right. Contour interval was 1 cm)

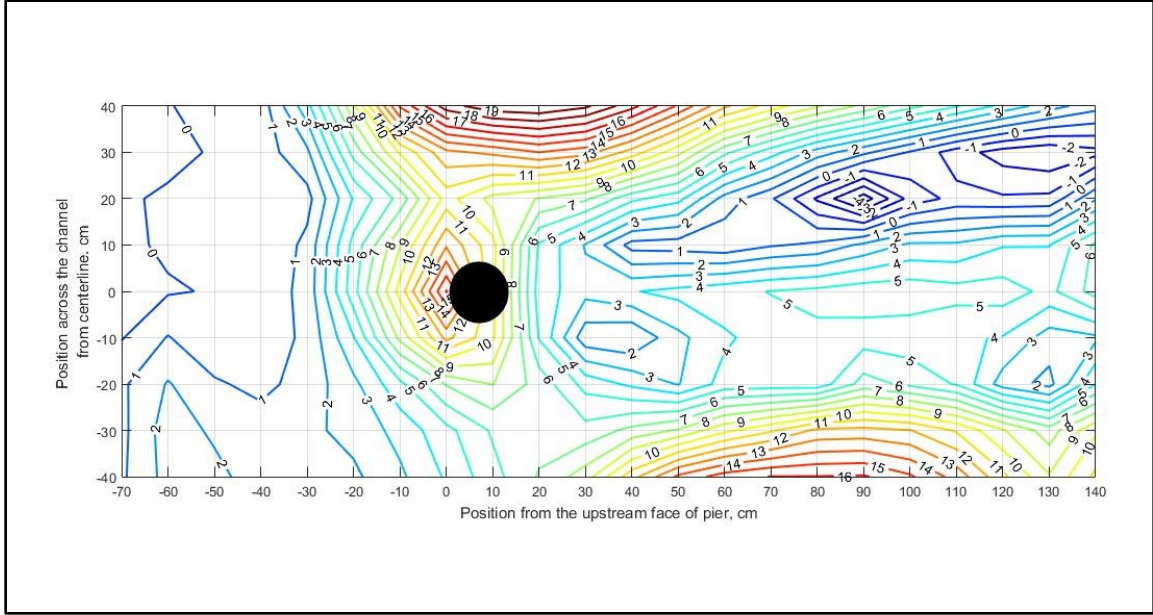


Figure 18. Bed profile for $V_a/V_w = 99.92$. (Flow was from left to right. Contour interval was 1 cm)

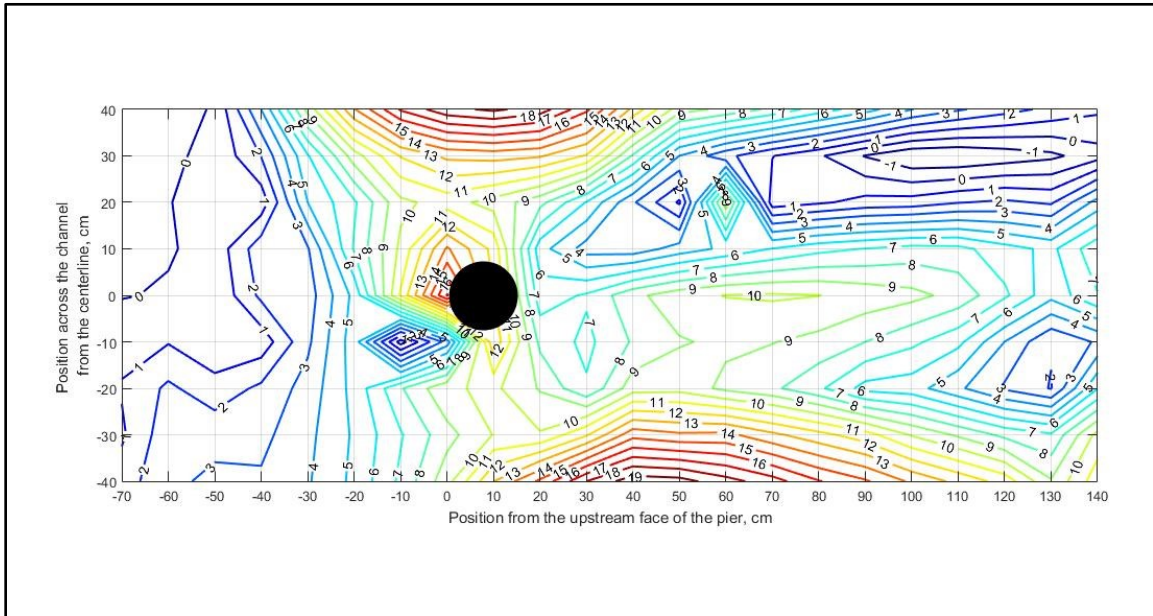


Figure 19. Bed profile for $V_a/V_w = 114.20$. (Flow was from left to right. Contour interval was 1 cm)

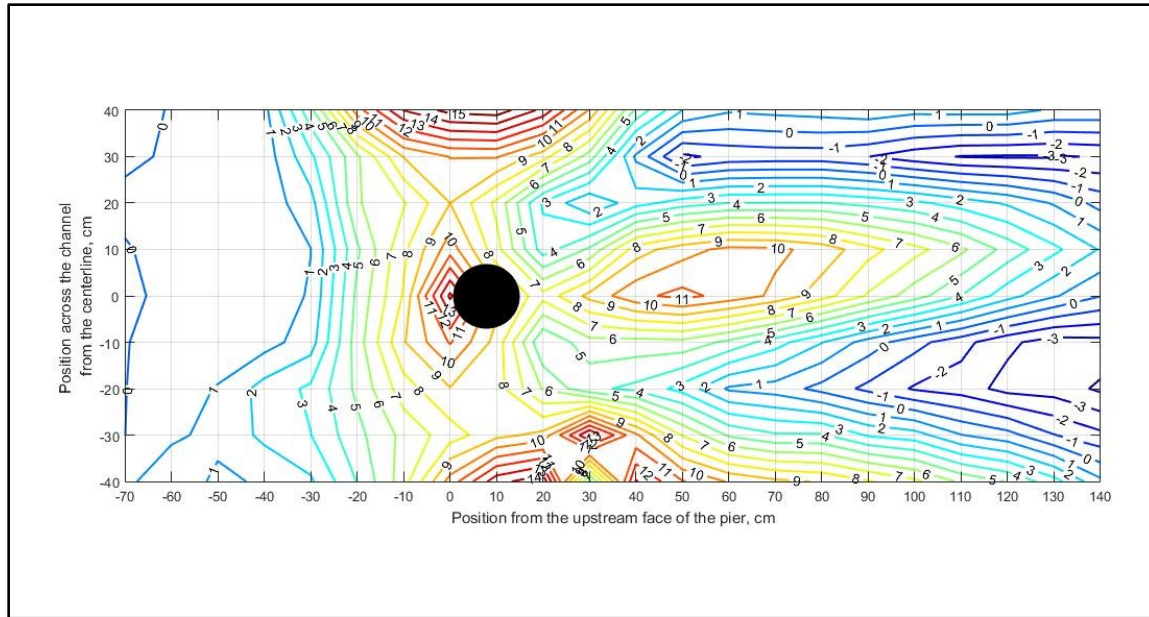


Figure 20. Bed profile for $V_a/V_w = 142.75$. (Flow was from left to right. Contour interval was 1 cm)



a) $V_a/V_w = 0$



b) $V_a/V_w = 7.15$



c) $V_a/V_w = 21.41$



d) $V_a/V_w = 35.68$



e) $V_a/V_w = 49.96$



f) $V_a/V_w = 71.37$



g) $V_a/V_w = 78.51$



h) $V_a/V_w = 85.65$



i) $V_a/V_w = 99.92$



j) $V_a/V_w = 114.20$

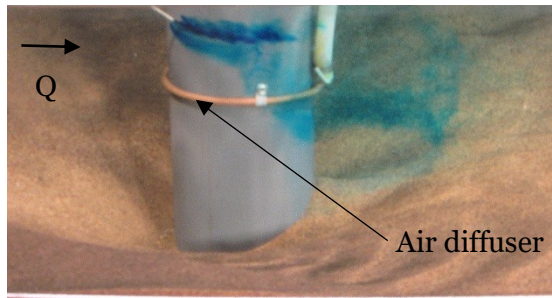
Figure 21. Plain view bed profile photos from a through j resulting from varied air flow rate represented by ratio of air velocity to water flow velocity V_a/V_w (Flow was from left to right)

Examining the bed profiles indicate a shift in flow direction from the center of the channel to sides as the air flow rate increases (**Figure 9** **Figure 10** - **Figure 21**). It can

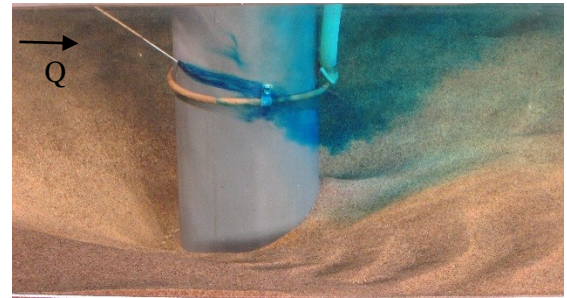
also be observed that the change in sediment pattern downstream of the pier indicates a possible horizontal vortex formation in the pier wake. This was confirmed by video-graphic evidence where the air bubbles went downward in the downstream section. This explains the formation of two crests on each side of the pier as seen in **Figure 21** **Figure 21(f–j)**. The two horizontal wake vortices create a counter vortex that bounces off the side wall and creates a scour hole on the channel sides (**Figure 14 - Figure 20** **Figure 21**).

3.7. Dye Test

The dye was introduced on the upstream face of the pier and the documented results are shown for the base case with no air injection (**Figure 22**) and with an air flow rate corresponding to $V_a/V_w=71.4$. (**Figure 23**).



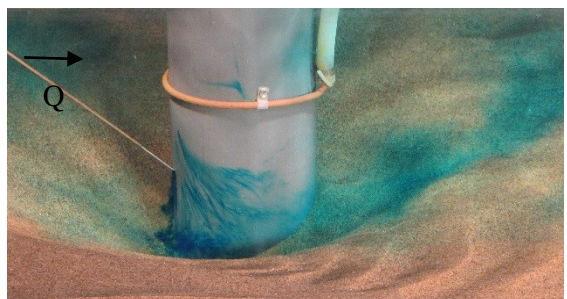
(a)



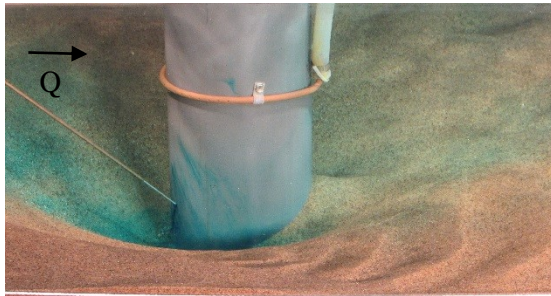
(b)



(c)

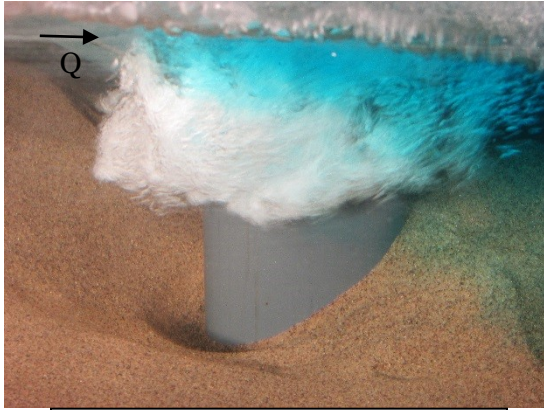


(d)

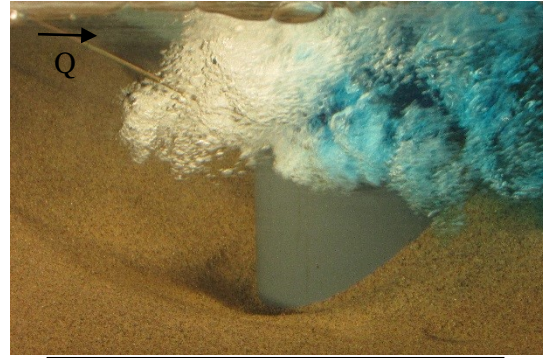


(e)

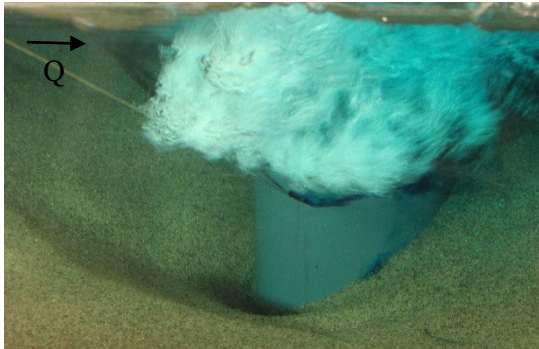
Figure 22. Side view of the flume with dye introduced at different positions for the base case ($V_a/V_w = 0$) (Flow from left to right)



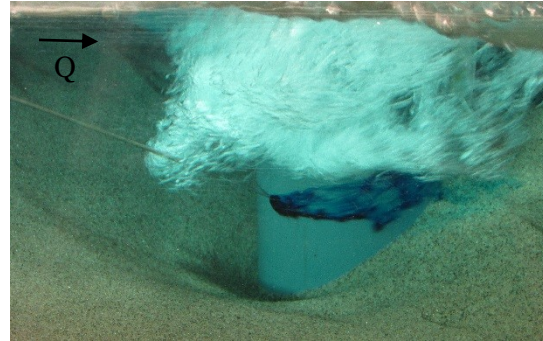
(a)



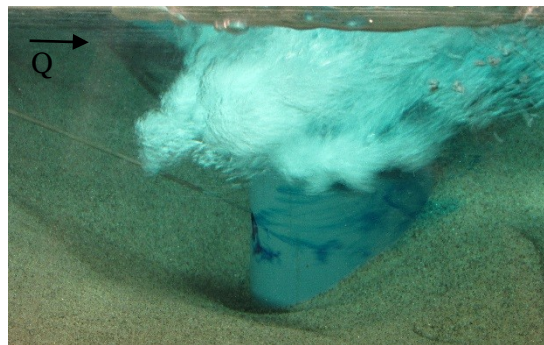
(b)



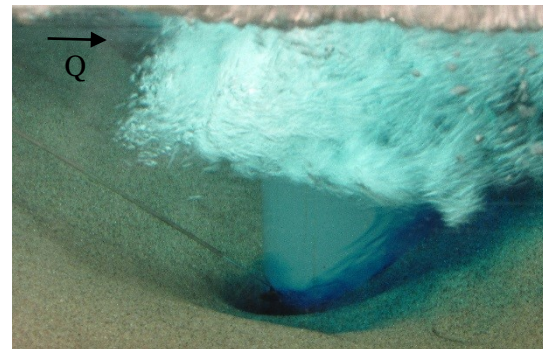
(c)



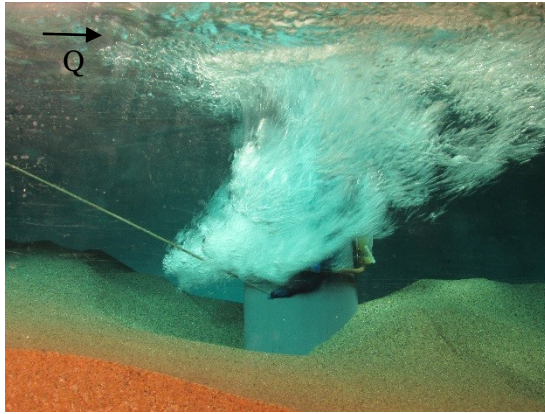
(d)



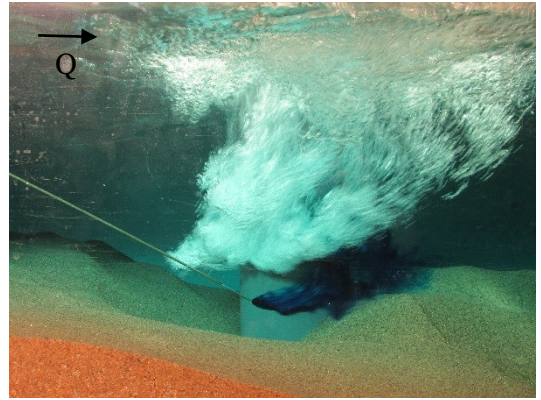
(e)



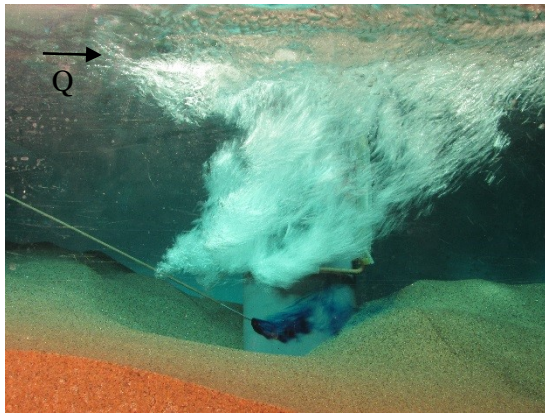
(f)



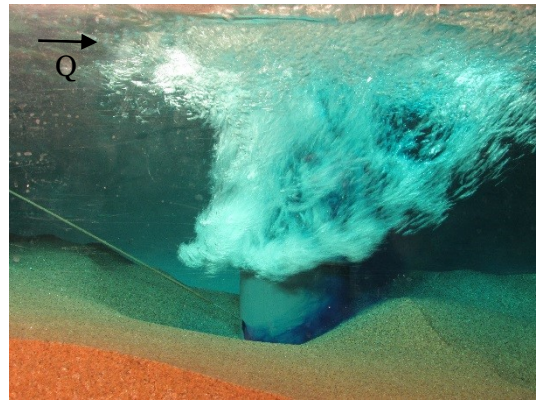
(g)



(h)



(i)



(j)

Figure 23. Side view of the flume with dye introduced at different positions for $V_a/V_w = 71$ (Flow from left to right. Air diffuser hidden by bubbles.)

A comparison of the photographs **Figure 22(c)** and **(d)** with that of **Figure 23 (d)** and **(e)** reveals a shift in the flow lines across the pier. In the first case without air, the flow lines are more flat and in the case with air, the flow lines are angled slightly upward. This indicates a change in flow behavior that was expected to contribute towards reducing the scour.

Chapter 4: Conclusions

In conducting the experiments to determine the effectiveness of air injection as a scour countermeasure at cylindrical bridge piers the following conclusions can be made:

1. The rate of scour follows asymptotic trend, increasing with an increasing air velocity ratio in the initial stages(**Figure 4**)
2. The maximum scour depth (**Figure 5**) and centerline scour depth (**Figure 6**) at equilibrium decrease with an increase in air flow velocity ratio up to a value of $V_a/V_w = 57.1$ and increases with a further increase in velocity ratio. The least scour of d_s/d_{so} of 0.67 (a reduction of 33%) occurred at $V_a/V_w=57.1$.
3. The time to reach equilibrium reduces with increase in air flow rate with limited scatter (**Figure 7**).
4. The water surface elevation along the centerline increases with an increase in air flow rate and the increase is inversely proportional to the distance from the upstream face of the pier (**Figure 8**).
5. The bed profile shows more sediment accumulation/ less scour in the pier wake with increasing air velocity (**Figure 9 - Figure 20**). The bed profile also shows a change in sediment pattern downstream indicating a change in flow behavior with increasing air flow (**Figure 21**).

Chapter 5: Future Work

Air injection has potential to be an effective countermeasure. Further research is needed to establish in-depth understanding the phenomenon. Some recommendations for future research are provided below.

1. More detailed velocity measurements using ADV are needed to document and understand the nature and scale of the effect air injection has on flow behavior.
2. This study presents the effect of air flow rate alone on the scour reduction efficiency. Other parameters such as air diffuser elevation, angle of air injection with respect to down flow, size, number and density of holes in air diffuser pipe and angle of coverage with respect to pier circumference could be varied to understand the effect of these factors on efficiency and derive an optimal configuration that incorporates all the parameters mentioned above.
3. In the cases with higher air flow rate, scour on the sides of the channels was higher compared to the base case with no air. A further study is recommended to examine the effects of air injection in wide channels on possible bank erosion and the interaction of air injection from other piers in the channel.
4. This study measured scour in terms of the maximum depth of local scour at the base of the pier. A study is recommended to examine the total volume of scour in the channels as air injection can impact channel aggradation or degradation.
5. In addition to the single pier studied here, a study on scour at multiple-pier configurations is recommended.

References

- Barkdoll, Brian D., and Casey J. Huckins. 2012. "The Role of Bridge Scour in Relation to Stream Restoration." *World Environmental and Water Resources Congress* . Albuquerque, New Mexico, United States: ASCE. 2546-2555.
- Champagne, Ted M., Rachael R. Barlock, Santosh R Ghimre, Brian D. Barkdoll, Juan A. Gonzalez-Castro, and Larry Deaton. 2016. "Scour Reduction by Air Injection Downstream of Stilling Basins: Optimal Configuration Determination by Experimentation." *Journal of Irrigation and Drianage Engineering* 1-9.
- Chiew, Yee-Meng. 2004. "Local Scour and riprap Stability at Bridge Piers in a Degrading Channel." *Journal of Hydraulic Engineering* 218-226.
- Chiew, Yee-Meng. 1992. "Scour Protection at Bridge Piers ." *Journal of Hydraulic Engineering* 118(9): 1260-1269.
- Chiew, Yee-Meng, and Foo-Hoat Lim. 2000. "Failure Behavior of Riprap Layer at Bridge Piers Under Live-Bed Conditions." *Journal of Hydraulic Engineering* 43-55.
- Chiew, Yee-Meng, and Siow-Yong Lim. 2003. "Protection of bridge piers using a sacrificial sill." *Water and Maritime Engineering*. Institute of Civil Engineers. 53-62.
- Dugue, Violaine, Ph.D., Koen, Ph.D. Blanckaert, Qiuwen Chen, and Anto J. and Schleiss. 2015. "Influencing Flow Patterns and Bed Morphology in Open Channels and Rivers by means of an Air-Bubble Screen." *Journal of Hydraulic Engineering* 141(2):-1--1.
- Grimaldi, Carmelo, Roberto Gaudio, Francesco Calomino, and Antonio H Cardoso. 2009. "Countermeasures against Local Scouring at Bridge Piers: Slot and Combined Sysytem of Slot and Bed Sill." *Journal of Hydraulic Engineering* (ASCE) 135 (5): 425-431.
- Harrison, Lawrence J. 1992. "Magnitude of The Scour Evaluation Program." *Hydraulic Engineering: Saving a Threatened Resource - In Search of Solutions*. Baltimore, MD: American Society of Civil Engineers.

- Isbash, S.V. 1935. *"Construction of Dams by Dumping Stones In Flowing Water"*
Translated by A. Dovjikov. Eastport, Maine: United States Engineer Office,
Engineer Division.
- Koloseus, Herman J. 1984. "Scour Due to Riprap and Improper Filters." *Journal of
Hydraulic Engineering* 110(10): 1315-1324.
- Lagasse, P F, P E Clopper, L W Zevenbergen, L G Girard, and Transportation Research
Board. 2007. *Countermeasures to Protect Bridge Piers from Scour*. National
Cooperative Highway Research Program Report 593, Washington:
Transportation Research Board.
- Lauchlan, Christine S., and Bruce W. Melville. 2001. "Riprap Protection at Bridge Piers." *Journal of Hydraulic Engineering* 412-418.
- Melville, Bruce W., and Anna C. Hadfield. 1999. "Use of Sacrificial Piles as Pier Scour
Countermeasures." *Journal of Hydraulic Engineering* 1221-1224.
- Moncada-M, A.T., J Aguire-PE, J.C. Bolivar, and E.J. Flores. 2009. "Scour protection of
circular piers with collars and slots." *Journal of Hydraulic Research* 119-126.
- Parola, A. C., Jr, and J. S. Jones. 1991. "Sizing Riprap to Protect Bridge Piers from
Scour." *Transportation Research Record* (1290), 276-280.
- Red FLint Sand & Gravel, LLC. Eau Claire,WI. 2008. "Particle Size Distribution Report."
12 20.
- Tafarojnoruz, Ali, Roberto Gaudio, and Francesco Calomino. 2012. "Evaluation of Flow-
Altering Countermeasures against Bridge Pier Scour." *Journal of Hydraulic
Engineering* 297-305.
- Worman, Anders. 1989. "Riprap Protection Without Filter Layer." *Journal of Hydraulic
Engineering* 115 (0733-9429/89/0012): 1615-1630.
- Yoon, Tae Hoon. 2005. "Wire Gabion for Protecting Bridge Piers." *Journal of Hydraulic
Engineering* 942-949.
- Yoon, Tae Hoon, and Dae-Hong Kim. 2001. "Bridge Pier Scour Protection by Sack
Gabions." *World Water Congress* . Orlando, Florida: ASCE.